Battery Charging Monitoring System Using PZEM 004t Sensor and DC Voltage Sensor

Musaddak Maher Abdul Zahra [*+], Hairder Sharif [**], Karam Myaser Abd Alazi[***], Nada Qasim Mohammed [****], Ahmed Abd Ali [*****], Hayder Tariq [******], Mohammed Qassim Mohammed [*******]

*+ Computer Techniques Engineering Department, Al-Mustaqbal University College, Hillah, Iraq

** College of Medical Technology/ Medical Lab techniques, ; Al-Farahidi University/Iraq

*** AlNoor University College, Bartella, Iraq

**** Al-Nisour University College/Iraq

***** College of Petroleum Engineering, Al-Ayen University, Thi-Qar , Iraq

****** Department of Pharmacy, Al-Zahrawi University College, Karbala, Iraq

******* Al-Esraa University College, Baghdad, Iraq

(786musaddak@gmail.com, Sharif45672@gmail.com, alaziz7862265@gmail.com, Mohammed564254@gmail.com, Tariq546225@gmail.com, Mohammed6872683@gmail.com)

‡Corresponding Author; Musaddak Maher Abdul Zahra, Computer Techniques Engineering Department, Al-Mustaqbal University College, Hillah, Iraq, Tel: +96 7829975667, 786musaddak@gmail.com)

Received: 24.04.2023 Accepted:26.05.2023

Abstract- Solar panels are designed to convert solar energy into electrical energy. This electrical energy is then sent to a battery or an inverter, which converts it into usable power. The power produced by the panels cannot be monitored directly as it is being generated. This system typically consists of a solar panel monitoring device that measures the voltage, current and temperature of the solar panel. This data is then used to determine the efficiency of the solar panel and identify any potential problems that need to be addressed. Monitoring the performance of the solar panel, it helps to ensure it is operating at its peak efficiency and reducing the risk of potential damage. A 100 Wp panel and a 12V 45 AH battery are used in the solar power plant battery charging process. The voltage sensor needs to be calibrated so that it can accurately measure the voltage from the solar panel and the battery. This is important because the voltage must be within certain parameters in order for the battery to charge safely and efficiently. By monitoring the performance of the solar panel and the voltage sensor, potential risks of damage can be minimized. Calibration is followed by determining the programme and low and high values. Using the Arduino IDE software, the programme is then input into Arduino. The results of the DC voltage sensor measurement and the programme used were then compared. A 3-day monitoring process is carried out for PLTS battery charging. The average voltage that rises during charging from 08.00 to 15.00 is 0.341 V after the monitoring process.

Keywords: battery, solar cell, monitoring system

1. Introduction

Electronic devices are mainly powered by electricity in the community. Among the many technological advances in the field of electricity today, it is no wonder that there is such a wide range of applications that meet the needs and demands of the community in terms of electrical energy [1]. The majority of electricity used today comes from fossil fuels (non-alternative energy). It is inevitable that fossil fuels will be depleted sooner or later. All the country has a lot of fossil fuels and renewable energy resources that can be utilized for generating electricity [2]. There has been a significant amount of progress in developing renewable energy sources. Solar Power Plant (PLTS) is one method of utilizing solar

thermal energy as a source of electrical energy [3]. There is a rapid expansion of PLTS, which will be able to produce 35 MW of electrical power in the near future. Furthermore, solar energy sources can also be used as a backup power source for homes, offices, government buildings, and can also be used in conjunction with PLN electricity to serve as the main source of electricity for homes, offices, and government buildings [4]. There is no state electricity company located in this area, because it is because of the location of the area that it is impossible to access the electricity network from the State Electricity Company (PLN). The use of solar PV in remote areas is one way to provide electricity to those areas [5]. Solar cells are thought to have a great deal of potential due to the low electrification rate. The use of a solar power plant (PLTS) with a modular system that is portable as an alternative means of generating power can be seen as a solution as an alternative power source [6]. A solar panel is a device that converts direct current from solar energy into a form that can be used in the home. This modern technology has several advantages, including ease of maintenance, cleaning, savings, and ease of installation. There is a need for a tool to monitor the performance of solar panels and provide notifications when a solar panel malfunctions so that damage to the panels is avoided and the efficiency of solar panels is decreased [7]. The PLTS has a monitoring system that can display the voltage and current produced by the panels. However, this system still has deficiencies, namely that it does not have a noise monitoring and notification system that might lead to a reduction in the performance of solar panels, especially when it comes to air quality [8]. It has been shown in previous research that solar power plants still require significant short-term investments and that they can only provide half a day's worth of electricity from the absorption of sunlight for a single day, thus requiring expensive short-term investments [9]. The optimum use of solar energy for households, however, is still determined by the intensity of sunlight. Solar panels' efficiency can also be affected by varying loads. There have also been studies in which the angle of solar panels was adjusted to get an optimum intensity of irradiation to be received by the panels [10]. The planning and analysis of solar home systems (SHS) for residential solar power generation systems. A solar home lighting system is one of the solar power systems used for rural electrification, with an installed power of 4855 watts. A total of 50 Wp is produced per household to meet lighting and information requirements [11]. The Arduino microcontroller-based solar power plant monitoring system monitors the current and voltage of solar panels to obtain current, voltage, and power values with data automatically stored on an SD card. Data on panel output parameters are only collected using this method [12]. It is, therefore, necessary to make a solar panel charging monitoring system with calibrated sensors so that the data acquisition system can be integrated with the Arduino UNO 328 microcontroller-based system so that it can be accessed in real-time [13]. The battery is a device that uses an electrochemical process to convert electrical energy into chemical energy when it is charged and then converts chemical energy back into electrical energy when the battery is discharged. The battery life of a smartphone can be rapidly shortened if it is charged and discharged improperly [14]. Therefore, it is necessary to monitor the battery in order to pay special attention to these two processes in order to maintain the battery's life. It is very important to keep an eye on the state of charge of a battery since it is one of the most important indicators [15]. An expression of the state of charge of a battery, known as SOC (State of Charge), is understood as the full amount of energy capacity that can be stored and utilized by a battery with its total capacity expressed as a percentage. Battery capacity is expressed as a percentage when describing available energy. In order to monitor the charging process of solar panel batteries, the researcher designed a system that uses a DC voltage sensor to monitor the charging process of solar panel batteries [16]. As the battery is being charged, the voltage sensor will take measurements of the voltage increase and the capacity of the battery during the charging process, which will be displayed on the LED as a reference when charging the battery. The battery is composed of two electrodes, an anode and a cathode, and an electrolyte that allows ions to move between the anode and cathode. When the battery is charged, the anode releases electrons which flow through the external circuit and back to the cathode. This creates a flow of ions from the anode to the cathode, storing energy in the form of chemical bonds. When discharged, the process is reversed, releasing the stored energy as electrical energy. Charging and discharging the battery causes the ions to move back and forth, which creates internal stress on the battery and causes the chemical bonds to break down. This can lead to decreased performance, shorter life span, and even explosions if the battery is overcharged. Overcharging and discharging the battery can cause the ions to move too fast and too often, leading to the buildup of heat. This heat can cause the battery to degrade over time, as it breaks down the chemical bonds and can even cause the battery to overheat and explode. Monitoring the battery is essential to keep it functioning properly and to avoid any potential damage. When a battery is consistently exposed to high temperatures, the chemical components deteriorate more quickly. This reduces the battery's charge capacity, leading to a shorter lifespan. Additionally, heat can cause the battery to swell and increase the risk of explosion. Monitoring the state of charge helps to ensure the battery is not overcharged and can detect when the battery is deteriorating. The State of Charge is expressed as a percentage and is determined by the charge level of the battery compared to the total capacity of the battery. The higher the percentage, the higher the amount of energy that can be used. The State of Charge is important because it gives an indication of how much energy is available to be used in the battery. A higher SOC means more energy is available, and a lower SOC means less energy is available. This helps users know when they need to recharge the battery.

2. Methods

In this study, the PLTS battery charging monitoring system is designed and manufactured to monitor the battery charging process on solar panels through a voltage sensor. With this system, the user can monitor the voltage of the solar panel battery, as well as the amount of current being drawn from the panel. This allows the user to understand the performance of the battery charging process, and make adjustments as needed to optimize the efficiency of the

system. The voltage sensor measures the voltage increase and battery capacity during the charging process and displays them on the LED as a reference. As the battery charges, the voltage increases [17]. The voltage sensor measures the rate of change in the voltage and the capacity of the battery to determine when the battery is fully charged. This information is then displayed on the LED to provide an accurate reading of the charging process. The circuit schematics and mechanical design of the device were created using several software tools. Figure 1 illustrates the circuit diagram of this device created using Proteus software. The PZEM sensor has a set of input pins as well as a set of output pins for RX and TX. It is a PZEM sensor that is attached to Arduino pin 11 for the TX pin and Arduino pin 12 for the RX pin when using the Arduino board [18]. The LCD pin has two i2c communication pins, SDA and SCL, which are connected to the Arduino SDA and SCL pins. An Arduino A0 pin is connected to the DC voltage sensor. A circuit simulation model simplifies the process of making tools and determines how component pins interact.

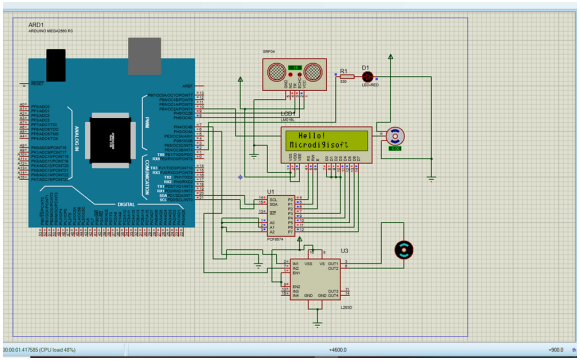

Fig.1. Schematic of the device

Fig. 2. Hardware prototype

The mechanical design of the tool is made using Sketchup software. The size of the mechanical design is 15 cm long, 12 cm wide, and 12 cm high. The material to be used is acrylic material with a thickness of 2 mm. Figure 2 shows the hardware prototype. The data collected was obtained in the form of sensor readings displayed by LEDs over three charging days of eight hours each. During battery charging, the readings displayed showed the DC voltage as well as the available battery capacity [19]. Once the data was collected, it was further processed and analysed to ascertain the findings of the sensor readings. The average value of voltage increase during battery charging can be calculated based on equation (1).

The average increase in voltage = (the amount of difference in voltage)/(charging time) -------- (1)

Testing DC voltage is carried out to verify the sensor performance and determine errors in the sensor results. Sensor readings are compared with measurements taken on the measuring instrument to determine the proportion of sensor readings that are inaccurate [20]. Equation (2) shows how to calculate the percentage difference between the sensors between the measuring instrument and the sensor tested.

Tool failure value = (measuring instrument readings – sensor readings)/(measuring instrument readings) X 100%

------ (2)

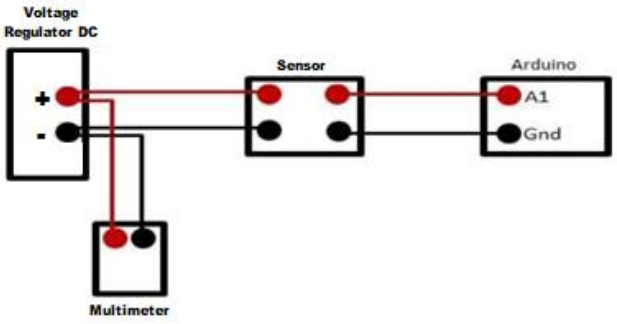

Fig. 3. DC sensor test circuit

Figure 3. illustrates the circuit schematic for testing this sensor. As shown in the diagram, the circuit consists of a power source, a voltage regulator, a voltage divider, a transistor, a sensor, and an LED. The power source is connected to the voltage regulator and then to the voltage divider, which regulates the voltage going to the transistor. The transistor is connected to the sensor, and the output of the sensor is connected to the LED. The LED is used to indicate when the sensor is activated [21]. The first step in testing the sensor is to connect it to the power supply. After connecting the power supply, the voltage regulator should be adjusted so that the voltage being sent to the voltage divider is within the range required to activate the sensor. Once that is done, the LED should be illuminated when the sensor is activated, indicating that the circuit is working properly. This test is carried out with a voltage of 0-20 volts DC and is done using the tested method. The second step involves connecting both the sensor and multimeter to the power supply [22]. The sensor readings and multimeter readings will then be compared to determine if the sensor is operating correctly. A mapping program was used to determine the percentage of battery capacity charge during testing. The software determines the minimum and maximum values for a given value. A low value represents the voltage of the battery when the inverter cannot be powered and a high value represents the battery's voltage when fully charged. During the charging process, the DC voltage sensor reading is automatically used to calculate the percentage of the battery based on low and high values [23]. The 100 Wp solar panel was also tested, as well as the DC voltage sensor and mapping program. Battery voltage is measured by a voltage sensor as the solar panel begins charging the battery. The battery is measured every hour until it is fully charged to determine how much charge it has left. The voltage sensor will not be connected in advance in order to avoid data collection problems during charging. Generally, a solar panel

with a capacity of 100 Wp will be powered by four batteries. It is usually expressed as a percentage of the battery's depth of discharge (DoD). A battery with a DoD of 80%, for example, allows 80% of its energy to be used, while 20% is held as a reserve. Solar panels that use four batteries are assumed to be in 100% condition [24]. According to the results of this study, the panel worked at 25% during testing when a single battery was used. During operation, the solar power plant outputs voltage and current as it charges the solar panel battery, which receives solar energy and converts it into electrical energy. The controller between the solar panel and battery regulates or continues the output current from the panel when charging occurs. The current then enters the battery through the controller, causing the battery voltage to gradually increase after the current enters the battery [25]. The battery condition will be checked every hour during battery charging until the battery is fully charged.

3. Results and Discussion

The initial voltage value of charging the battery and the final voltage value after the battery reaches full capacity should be determined before charging the battery. This study obtained an initial charging voltage value of 11.38 V and a final charging voltage value of 14.11 V. The battery capacity rating, as far as the battery is concerned, ranges from a rating of 78% - 100%. The DC voltage sensor readings were obtained for three days after the monitoring process was completed when charging the battery [26].

3.1 Day one report of DC voltage

The initial voltage of the battery before charging is 11.38 volts, as shown in Table 1. Battery voltage rating is the value when the battery can no longer supply the inverter with power. The battery voltage rose to 12.55 V after one hour of charging, with a difference of 1.71 V compared to the battery voltage before charging. The battery voltage increased in the same manner as the reading at 09.00 - 10.00 WIB at 11.00 - 12.00 WIB. It has been observed that the peak time of solar irradiation (watt peak) does not influence the charging process for 4 hours [27]. The battery's percentage value increases due to the voltage reaching 13.01 volts, resulting in an increase in the percentage value. Table 1 compares the sensor voltage ratings. When the voltage rating on the battery is still 12 volts at 09.00-11.00 WIB, the battery percentage is not affected. If the voltage rating on the battery changes dramatically enough, the battery percentage will change. A graph of the magnitude of the increase in battery voltage is shown in Figure 4, and it is clear that the greatest value occurs between 08.00 and 09.00 WIB, or when the batteries are charging for the first time, at 1.17 volts. However, for the duration of 09.00 WIB until 12.00 WIB, the voltage that increases is fairly the same as it does for the rest of the night, between 0.19 V and 0.08 V respectively [28]. According to researchers, this is caused by an increase in solar panel temperature. The results are in agreement with previous research findings that about 0.5% of the total power is generated [9]. When the readings are taken at 1:00 p.m., this is also reinforced. The large increase in battery voltage is quite significant when compared with 1:00 p.m. readings 9.00 WIB until 12.00 WIB. The sun's heat is diminishing at 13.00 WIB, and the panel's temperature is also decreasing. When determining the percentage of battery capacity calculated by the mapping program, it is important to review the calculation, because if the voltage value rises quite high during the first and fourth-hour readings, the percentage of the battery that is read will change [18]. According to equation (1), the battery voltage increased by 0.341 volts on the first day of testing.

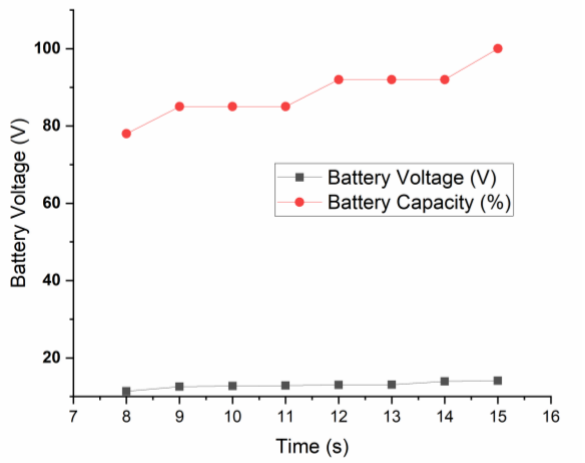

Fig. 4. Day 1 Variation of battery voltage and capacity with time

3.2 Day two report of DC voltage

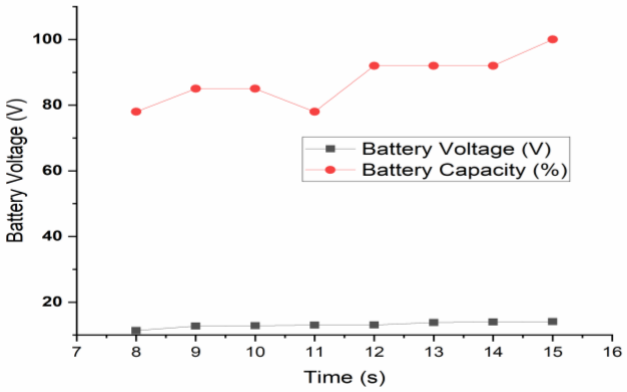

Fig. 5. Day 2 Variation of battery voltage and capacity with time

Table 2 shows the results of the DC voltage sensor readings on the second day. The battery voltage rose to 12.74 V after 1 hour of charging with a difference of 1.36 V compared to its initial voltage value before charging with a 7% increase in voltage. During the battery charging process, the weather turned cloudy at 10:00-11:00 WIB, which obviously impacted the solar panel's performance [16]. The increase in voltage in the battery at 11:00 -12:00 WIB is the same as that at 09:00 - 10:00 WIB. It is due to the peak of sunlight (watt peak) still occurring between 12:00 and 13:00 WIB that battery voltage increases. The solar panel started to charge the batteries optimally after six hours, based on the readings taken at that time. The graph in Figure 5 of the voltage increases shows that the greatest percentage increase in voltage occurs between 8.00 and 09.00 WIB or during the first hour of charging at 1.36V. The lowest voltage increase occurred between 09.00 - 10.00 WIB. This is related to the

sun having entered its first peak when the solar panel should produce peak wattage based on its ability and capacity. In the graph of voltage readings at this second hour, it can be seen that the peak sun peak has little or no impact on battery charging [14]. According to equation (2), the average voltage increase on the second day of testing was the same as the previous day.

3.3 Day three report of DC voltage

Table 3 shows the DC voltage sensor readings on the third day of testing. As shown in Figure 6, the largest voltage increase occurs at 08.00 - 09.00 WIB or at 1.36 for the first hour of charging. According to the fourth-hour reading (10:30 -11:00 WIB), the lowest value was obtained at 10:00 - 11:00 WIB. The battery voltage sensor reading value increased from 12.87 V to 12.94 V in the fourth hour [21]. There has been no change in the percentage of the battery since 12 V is still the voltage value. A large change in the voltage rating will result in a change in battery percentage. The battery charging process was carried out over three days in different weather conditions. It has been found that solar panels can be effectively illuminated by sunlight for 9 hours, starting at 07.00 WIB and ending at 17.00 WIB. A battery may not fully charge in a day because of various factors, including clouds and rain. According to the data, the biggest voltage increases always occurred during the first hour of charging, and then the voltage decreased until the battery was fully charged [8]. This tool entered the high and low battery charge ratings into the software that will be fed into the device, even though the results of the DC voltage sensor tested were good enough. The sensor and battery are connected during the battery charging process after the sensor and software have been calibrated. In this study, the battery voltage measured when it cannot supply the inverter is 11.38 V, while the battery voltage measured when the battery is at full capacity is 14.11 V. The voltage rating of the battery should be checked for more accurate readings [12]. The voltage sensor reading is then compared with the measurement instrument value for a more accurate reading. Table 3 shows the error/error value for the reading sensors. According to Table 3, the largest error rating is 0.228% for a difference of 0.03 between sensor reading and measuring instrument measurement. Table 3. shows an average error of 1.875% based on the data.

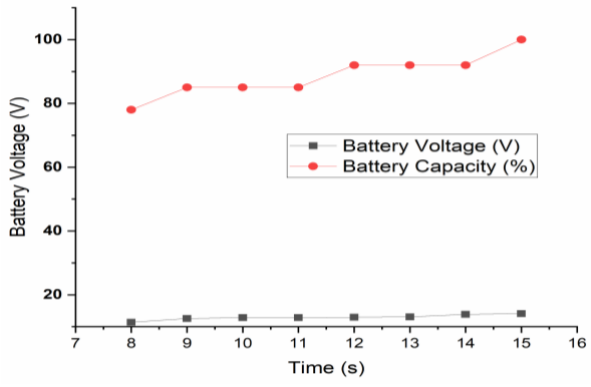

Fig. 6. Day 3 Variation of battery voltage and capacity with time

4. Conclusions

A battery charging monitoring system such as the 100Wp PLTS battery charging monitoring system that uses a DC voltage sensor can be configured to give accurate readings if the DC voltage sensor has been calibrated before use after the calibration process has been completed. The DC voltage sensor measures the amount of voltage being sent to the battery and is used to detect when the battery is fully charged. By calibrating the sensor before use, it can detect the exact voltage that the battery needs to be charged to and indicate when the battery is fully charged. The sensor must be connected to Arduino which has been programmed to work properly with a fairly small reading error in order to display reading results. When the battery is being charged, the DC voltage sensor measures the exact amount of voltage being sent to the battery, and then sends the data back to Arduino. Arduino then compares the data to the calibrated voltage given to the sensor before use and determines whether the battery is fully charged with a fairly small reading error. DC voltage sensor readings are quite accurate, as shown by a comparison between sensor readings and measuring instruments, where no more than 1% of reading errors are observed. The number of batteries used for the PLTS should be at least four in order to achieve optimal performance. PLTS can use this information to support its performance when supplying the load.

References

[1] T. Long, Q.S Jia, G. Wang, and Y. Yang, "Efficient real-time EV charging scheduling via ordinal optimization," IEEE Trans. Smart Grid, vol.12, pp. 4029–4038, 2021.

[2] P. Sterchele, K. Kersten, A. Palzer, J. Hentschel, and H.M. Henning, "Assessment of flexible electric vehicle charging in a sector coupling energy system model—modelling approach and case study," Appl. Energy, vol. 258:114101, 2020.

[3] J.K. Szinai, C.J.R. Sheppard, N. Abhyankar, and A.R. Gopal, "Reduced grid operating costs and renewable energy curtailment with electric vehicle charge management," Energy Policy, vol.136:111051, 2020.

[4] R. Tu, J. Gai, Y. Jessie, B. Farooq, D. Posen, and M. Hatzopoulou, "Electric vehicle charging optimization to minimize marginal greenhouse gas emissions from power generation," Appl. Energy, vol.277:115517, 2020.

[5] M.H. Abbasi, M. Taki, A. Rajabi, L. Li, and J. Zhang, "Coordinated operation of electric vehicle charging and wind power generation as a virtual power plant: a multi-stage risk constrained approach," Appl. Energy, vol.239, pp.1294–1307, 2020.

[6] T. Chen, X.P. Zhang, J. Wang, J. Li, C. Wu. M. Hu, and H. Bian, "A review on electric vehicle charging infrastructure development in the UK," Power Syst. Clean Energy, vol. 8, pp. 193–205, 2020.

[7] P. Zhou, R.Y. Zhang, J. Xie, J.P. Liu, H. Wang, and Y. Chai "Data-driven monitoring and diagnosing of abnormal furnace conditions in blast furnace ironmaking: An integrated PCA-ICA method," IEEE Trans. Ind. Electron., vol. 68, pp. 622–631, 2021.

[8] S.K Mathew, and Y. Zhang, "Acoustic-based engine fault diagnosis using WPT, PCA, and Bayesian optimization," Appl. Sci. Basel, vol.10:6890, 2020.

[9] C. Qi, "Big data management in the mining industry," Int. J. Miner. Metall. Mater., vol. 27, pp. 131–139, 2020.

[10] R. Zhao, R.Q. Yan, Z.H. Chen, K.Z. Mao, P. Wang, and R.X. Gao, "Deep learning and its applications to machine health monitoring," Mech. Syst. Signal Process., vol. 115, pp. 213–237, 2019.

[11] C. Lu, and W. Li, "Fault diagnosis method of petrochemical air compressor based on deep belief network," CIESC J., vol. 70, pp. 757–763, 2019.

[12] W. Hui, S. Y. Guang, Z. Y. Qin, L. M. Kai, X. Meng, and Z.Y. Yuan, "The design and implementation of a service composition system based on a restful API," Intell. Autom. Soft Comput., vol. 25, pp. 573–583, 2019.

[13] C. Teng, C. Zhang, K. Yin, M. Zhao, Y. Du, Q. Wu, and X. Lu, "A new high-performance rechargeable alkaline Zn battery based on mesoporous nitrogen-doped oxygen-deficient hematite," Sci. China. Mater., vol.65, pp. 920–928, 2022.

[14] T. Wei, Y. Peng, L. Mo, S. Chen, R. Ghadari, Z. Li, and L. Hu, "Modulated bonding interaction in propanediol electrolytes toward stable aqueous zinc-ion batteries" Sci. China Mater., vol.65, pp.1156–1164, 2022.

[15] Y. Zhang, J. Li, L. Ma, H. Li, X. Xu, X. Liu. T. Lu and L. Pan, "Insights into the storage mechanism of 3D nanoflower-like V3S4 anode in sodium-ion batteries, J. Chem. Eng., vol.427: 130936,2022.

[16] H. Huang, L. Han, X. Fu, Y. Wang, Z. Yang, L. Pan, and M. Xu, A powder self-healable hydrogel electrolyte for flexible hybrid supercapacitors with high energy density and sustainability," Sml., vol.17: 2006807, 2021.

[17] Z. Tong, T. Kang, Y. Wan, R. Yang, Y. Wu, D. Shen, S. Liu, Y. Tang, and C. Lee, "A Ca-ion electrochromic battery via a water-in-salt electrolyte," Adv. Funct. Mater., vol.31: 2104639, 2021.

[18] S.C. Sekhar, B. Ramulu, S.J. Arbaz, S.K.K. Hussain. and J.S. Yu, "One-pot hydrothermal-derived NiS_2-$CoMo_2S_4$ with vertically aligned nanorods as a binder-free electrode for coin-cell-type hybrid supercapacitor," Small Methods, vol.5: 2100335, 2021.

[19] J. Li, L. Han, X. Zhang, H. Sun, X. Liu, T. Lu, Y. Yao and L. Pan, "Multi-role TiO_2 layer coated carbon@few-layered MoS2 nanotubes for durable lithium storage," J. Chem. Eng., vol.406: 126873, 2021.

[20] G. Nagaraju, S.C. Sekhar, B. Ramulu, and J.S. Yu, "High-performance hybrid supercapacitors based on MOF-derived hollow ternary chalcogenides," Energy Storage Mater., vol.35, pp.750–760, 2021.

[21] Y. Zhou, X. Tong, N. Pang, Y. Deng, C. Yan, D. Wu, S. Xu, D. Xiong, L. Wang, and P.K. Chu, "Ni_3S_2 nanocomposite structures doped with Zn and Co as long-lifetime, high-energy-density, and binder-free cathodes in flexible aqueous nickel-zinc batteries," ACS Appl. Mater. Interfaces, vol.13, pp.34292–34300, 2021.

[22] B. Safdar, A.K. Prasad, and K.S. Ahn, "NiCo-mixed hydroxide nanosheets as a new electrochromic material with fast optical response", Chem. Phys. Lett., vol.783: 139024, 2021.

[23] J. Li, Z. Ding, J. Li, C. Wang, L. Pan, and G. Wang , "Synergistic coupling of NiS1.03 nanoparticle with S-doped reduced graphene oxide for enhanced lithium and sodium storage," Chem. Phys. Lett., vol.407: 127199, 2021.

[24] M. Cui, X. Bai, J. Zhu, C. Han, Y. Huang, L. Kang, C. Zhi, and H. Li, "Electrochemically induced $NiCoSe_2$@NiOOH/CoOOH heterostructures as multifunctional cathode materials for flexible hybrid Zn batteries," Energy Storage Mater., vol.6, pp.427–434, 2021.

[25] Z. Tong, T. Kang, Y. Wan, R. Yang, Y. Wu, D. Shen, S. Liu, Y. Tang, and C.S. Lee, "A Ca-ion electrochromic battery via a water-in-salt electrolyte," Adv. Funct. Mater., vol.31: 2104639,2021.

[26] Y. Chen, J. Zhu, N. Wang, H. Cheng, X. Tang, K. Sand, and W. Hu, "Significantly improved conductivity of spinel Co_3O_4 porous nanowires partially substituted by Sn in tetra-hedral sites for high-performance quasi-solid-state supercapacitors," J. Mater. Chem. A, vol.9, pp.7005–7017, 2021.

[27] L. Wan, Y. Tang, L. Chen, K. Wang, J. Zhang, Y. Gao, J.Y. Lee, T. Lu, X. Xu, J. Li, Y. Zheng, and L. Pan, "In-situ construction of g-C3N4/Mo2CTx hybrid for superior lithium storage with significantly improved Coulombic efficiency and cycling stability," J. Chem. Eng., vol. 410:128349, 2021.

[28] J. Li, Z. Ding, L. Pan, J. Li, C. Wang, and G. Wang, "Facile self-templating synthesis of layered carbon with N, S dual doping for highly efficient sodium storage," Carbon, vol.173, pp. 31–40, 2021.

Table 1. Day one report of DC voltage			
Time	**Battery Voltage (V)**	**Battery Capacity(%)**	**Filling Description**
08.00	11.38	78	Initial condition
09.00	12.55	85	First condition
10.00	12.74	85	Second condition
11.00	12.82	85	Third condition
12.00	13.01	92	Fourth condition
13.00	13.09	92	Fifth condition
14.00	13.92	92	Sixth condition
15.00	14.11	100	Seventh condition

Table 2. Day two report of DC voltage			
Time	**Battery Voltage (V)**	**Battery Capacity(%)**	**Filling Description**
08.00	11.38	78	Initial condition
09.00	12.74	85	First condition
10.00	12.82	85	Second condition
11.00	12.99	78	Third condition
12.00	13.09	92	Fourth condition
13.00	13.82	92	Fifth condition
14.00	13.99	92	Sixth condition
15.00	14.11	100	Seventh condition

Table 3. Day two report of DC voltage			
Time	**Battery Voltage (V)**	**Battery Capacity(%)**	**Filling Description**
08.00	11.38	78	Initial condition
09.00	12.74	85	First condition
10.00	12.82	85	Second condition
11.00	12.99	78	Third condition
12.00	13.09	92	Fourth condition
13.00	13.82	92	Fifth condition
14.00	13.99	92	Sixth condition
15.00	14.11	100	Seventh condition